Photofragment translational spectroscopy of 1,2-butadiene at 193 nm

Jason C. Robinson, Weizhong Sun,[a] and Sean A. Harris
Chemical Sciences Division, Lawrence Berkeley National Laboratory, Berkeley, California 94720 and Department of Chemistry, University of California, Berkeley, California 94720

Fei Qi
Chemical Sciences Division, Lawrence Berkeley National Laboratory, Berkeley, California 94720

Daniel M. Neumark
Chemical Sciences Division, Lawrence Berkeley National Laboratory, Berkeley, California 94720 and Department of Chemistry, University of California, Berkeley, California 94720

(Received 18 July 2001; accepted 23 August 2001)

Photofragment translational spectroscopy has been used to investigate the dissociation dynamics of 1,2-butadiene at 193 nm. Ionization of scattered photoproducts was accomplished using tunable VUV synchrotron radiation at the Advanced Light Source. Two product channels are observed: $CH_3+C_3H_3$ and C_4H_5+H. The C_3H_3 product can be identified as the propargyl radical through measurement of its photoionization efficiency curve, whereas the C_4H_5 product cannot be identified definitively. The translational energy $P(E_T)$ distributions suggest that both channels result from internal conversion to the ground electronic state followed by dissociation. The $P(E_T)$ distribution for the C_4H_5 product is sharply truncated below 7 kcal/mol, indicating spontaneous decomposition of the slowest C_4H_5 product. © *2001 American Institute of Physics.* [DOI: 10.1063/1.1410975]

I. INTRODUCTION

Photodissociation studies offer a wealth of information regarding the disposal of energy by excited molecules or radicals.[1] Unsaturated hydrocarbon molecules are particularly interesting systems for study by this method. Compared to saturated hydrocarbons, they have a larger number of low-lying electronic states that can contribute to their spectroscopy and photodissociation dynamics. Multiple product channels are typically accessible upon UV excitation of these species, and in general several isomeric forms of the polyatomic fragments can be formed. Hence, the primary photochemistry of unsaturated hydrocarbons is of interest. Photodissociation experiments also probe important dynamical issues, including whether dissociation occurs on an excited state or the ground state surface and the extent to which isomerization occurs prior to product formation. The current study focuses on the 193 nm dissociation of 1,2-butadiene, an isomer of C_4H_6, under collisionless conditions. The issues that have been addressed here are the identities of the primary products from the dissociation event, the relative importance of different product channels, and the partitioning of available energy following bond cleavage.

Previously, the unimolecular dissociation of 1,2-butadiene has been investigated using mercury photosensitization,[2] VUV photolysis,[3,4] and shock tube pyrolysis.[5–7] All of these studies were carried out at relatively high pressure, such that multiple collisions took place during the course of the measurement. The VUV photolysis studies presented evidence for several competing reaction pathways, including methyl loss, sequential atomic hydrogen loss, molecular hydrogen loss, C_2H_2 loss, and methylene loss.[3,4] The thermal decomposition of 1,2-butadiene yielded $CH_3+C_3H_3$, which corresponds to breaking the weakest bond. Atomic hydrogen loss was insignificant in these studies. However, isomerization of the 1,2-butadiene to other forms of C_4H_6, such as 1,3-butadiene, 1-butyne, and 2-butyne, played an important role in the thermal studies.[6,7] Rate constants were derived for the decomposition of 1,2-butadiene to CH_3 and C_3H_3 radicals, as well as for the isomerization of 1,2-butadiene to 1,3-butadiene.

In our experiment, the technique of molecular photofragment translational spectroscopy has been used to identify the photofragments and ascertain their center-of-mass frame translational energy distributions. While many studies of this type have been carried out using electron impact ionization of the photofragments, extensive dissociative ionization from electron impact can complicate the analysis of hydrocarbon photodissociation, due to the large number of ionic fragments that can result from a single photodissociation channel. The experiments described here were conducted at the Advanced Light Source (ALS) at the Lawrence Berkeley National Laboratory, using a molecular beam photodissociation instrument in which the fragments are photoionized by tunable vacuum ultraviolet (VUV) synchrotron radiation rather than ionized by electron impact. Complications due to dissociative ionization are largely eliminated by tuning the photoionization energy below the dissociative photoionization threshold for a particular fragment, and in principle, one can identify a photofragment unambiguously by measuring its photoionization efficiency yield as a function of VUV energy, a particularly useful feature if multiple isomers are possible.

[a]Present address: AXT, Inc., Fremont, CA 94538.

We find two primary reaction channels for 1,2-butadiene, methyl loss and H atom loss, both of which are simple bond fission channels. Translational energy distributions were determined for both channels, and photoionization efficiency curves were measured for the C_3H_3 and C_4H_5 fragments. In addition, the branching ratio for the observed channels was calculated. The translational energy distributions indicate that dissociation occurs after internal conversion to the ground state, and that the most highly excited C_4H_5 fragments undergo secondary dissociation. No products attributable to isomerization to other C_4H_6 structures (such as 1,3-butadiene) are seen. The work here is the first of a series dealing with the photodissociation of C_4H_6 isomers, the other systems of interest being 1,3 butadiene and 2-butyne, with the overall goal of constructing a global picture of the dissociation dynamics and isomerization barriers that connect these species.

II. EXPERIMENT

The apparatus employed in this experiment has been described in detail elsewhere.[8,9] In brief, a pulsed molecular beam is crossed with a pulsed photolysis laser beam in a rotating source/fixed detector configuration. Scattered photofragments enter a multiply differentially pumped detection region where they are photoionized by VUV light from the ALS; the resulting ions are mass selected and detected. At a fixed scattering angle and VUV wavelength, the photofragment time-of-flight (TOF) distribution can be determined. Alternatively, the mass-selected ion yield as a function of VUV wavelength can be measured to determine the photoionization efficiency (PIE) curve for a particular fragment.

1,2-butadiene (97%) was obtained from Scott Specialty Gases and used without further purification. A pulsed molecular beam of ~5% 1,2-butadiene in either helium or neon was generated with a pulsed valve operating at 100 Hz. The stagnation pressure was maintained around 400 Torr using a vacuum regulator, and the pulsed valve was heated to approximately 60 °C to minimize the presence of dimers. The molecular beam was skimmed twice and crossed with 193 nm light emitted by a Lambda Physik LPX-200 ArF excimer laser. The laser beam was perpendicular to both the molecular beam and detector axes, and the molecular beam source could be rotated about the laser beam with respect to the fixed detector. Laser power was controlled to insure that the TOF spectra were not the result of multiphoton processes. For TOF studies, the laser was focused to a 2 mm×4 mm rectangle and laser pulse energy was maintained around 18 mJ/pulse. Shot-to-shot background subtraction was rendered unnecessary by choosing photoionization energies below the appearance potential of each species from the parent molecule.

Following dissociation, the neutral photofragments traveled 15.1 cm prior to ionization. Ionization of the scattered neutral photofragments was accomplished using tunable VUV undulator radiation from the Chemical Dynamics Beamline at the ALS. The ionized fragments were mass selected by a quadrupole mass filter, and the signal from the fragments of interest was counted as a function of time by a computer-interfaced multichannel scaler (MCS). An MCS bin width of 2 μs was used for all spectra presented here.

The properties of the VUV undulator radiation used in these experiments for photoionization of the dissociation products have been described previously.[10,11] The PIE measurements were conducted at 1.5 GeV electron beam energy, while the TOF spectra were collected using 1.9 GeV electron beam energy. The VUV photon flux is generally higher at 1.9 GeV, but at 1.5 GeV the useable VUV radiation range extends to a lower value, around 5 eV, which is more convenient for photoionization scans of radicals with low ionization potentials. The bandwidth of the radiation from the undulator is approximately 2.3%. The undulator radiation passes through a differentially pumped gas filter to remove the higher harmonics.[12] In these experiments, the gas filter was maintained at roughly 25 Torr of continuously flowing argon. While the upstream mirrors and the gas filter remove the higher harmonics of the undulator radiation, a small blue tail remains on the fundamental. To reduce the effects of this component of the radiation, an MgF_2 window, which transmits no light above 11.2 eV, could be inserted into the path of the undulator radiation. A calorimeter was employed to continuously monitor the VUV radiation flux.

Angle-resolved TOF profiles were obtained by selecting the mass-to-charge ratio (m/e) for the ion of interest, fixing the source angle, and setting the undulator gap to deliver the appropriate photoionization energy. TOF spectra were taken at multiple source angles for each m/e. Photoionization efficiency curves for specific photofragments were obtained by selecting m/e, fixing the source angle, and stepping the undulator radiation. In constructing the curve, the scattering signal for each fragment was integrated, background subtracted, and normalized.

III. RESULTS

A. TOF spectra

Figure 1 shows the accessible photodissociation channels for 1,2-butadiene at 193 nm (148.1 kcal/mol). Figure 1 was constructed using previously determined experimental and theoretical heats of formation;[13–20] values at 298 K were used for consistency. Product TOF spectra were collected for ions with $m/e=53$, 52, 39, 28, 27, 26, and 15. Only the TOF spectra for $m/e=53$, 39, and 15 showed clear evidence for primary dissociation channels, corresponding to the reactions

$$C_4H_6+h\nu\rightarrow C_3H_3+CH_3, \tag{R1}$$

$$C_4H_6+h\nu\rightarrow C_4H_5+H. \tag{R2}$$

TOF spectra for these three m/e values were taken at several laboratory angles. None of the other masses that were probed ($m/e=52$, 28, 27, 26) showed unambiguous evidence supporting any of the other possible primary dissociation pathways. Very small signal was seen at $m/e=52$, 27, and 26. To check for the presence of dimers in the molecular beam, TOF spectra at $m/e=54$ were collected at a source angle of $\Theta_{LAB}=7°$. However, no noticeable signal was detected. Signal was not collected for $m/e=1$ or 2 due to the poor kinematics associated with H and H_2 detection.

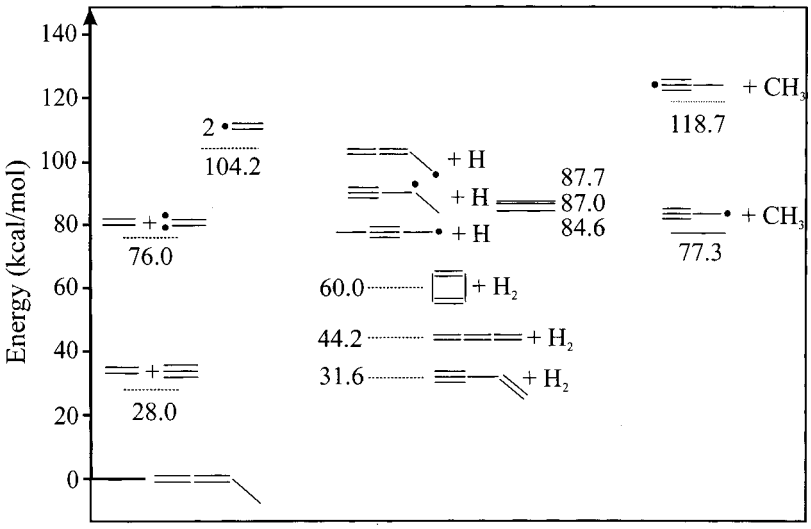

FIG. 1. Energy level diagram for the possible product channels following 193 nm excitation of 1,2-butadiene. Heats of formation (at 298 K) were taken from the literature. Solid lines indicate observed product channels, while dashed lines indicate products that were not observed. Solid black circles indicate radical sites.

For $m/e=39$ and 15, all TOF spectra were collected using molecular beams seeded in He, while TOF spectra for $m/e=53$ were obtained for Ne- and He-seeded beams. Figure 2 shows TOF spectra for $m/e=39(C_3H_3^+)$ at laboratory angles $\Theta_{LAB}=15°$ and 30°. These were collected at a photoionization energy of 11 eV, without the MgF_2 window. Additional spectra were collected at $\Theta_{LAB}=9°$, 20°, and 25°. Figure 2 also shows the TOF spectrum for the methyl radical ($m/e=15$) at $\Theta_{LAB}=15°$ and a photoionization energy of 11 eV.

TOF spectra for $m/e=53(C_4H_5^+)$ are shown in Fig. 3. These spectra were taken at a photoionization energy of 8.5 eV with the MgF_2 window inserted into the path of the undulator radiation. The TOF spectra at $\Theta_{LAB}=6°$ and 10° were taken using a He-seeded beam, while the spectrum at $\Theta_{LAB}=9°$ was taken with a Ne-seeded beam. The Ne-seeded beam provides more information on the slowest C_4H_5 products; for a He-seeded beam, these products are scattered at small laboratory scattering angles where they are obscured by the parent beam. Additional spectra (not shown) were taken at 8° with a He-seeded beam and 15° with a Ne-seeded beam.

B. PIE measurements

Figure 4 shows the photoionization efficiency (PIE) curves for the scattered C_3H_3 and C_4H_5 fragments taken at $\Theta_{LAB}=17°$ and 7°, respectively, with the MgF_2 window in place. The photoionization onsets are 7.8 ± 0.2 eV for C_3H_3 and 7.3 ± 0.2 eV for C_4H_5. However, the ''tails'' in the PIE curves extending to low photon energy are characteristic of hot bands from vibrationally excited neutrals, so the ionization potential (IP) of the fragment can be better (if still crudely) estimated by straight-line extrapolation of the PIE curve. This procedure yields IP's of 8.4 ± 0.2 eV for C_3H_3 and 7.5 ± 0.2 eV for C_4H_5. The value obtained for the C_3H_3 fragment indicates it is the propargyl radical, for which the IP has been determined by ZEKE spectroscopy to be 8.763 eV,[19] rather than another C_3H_3 isomer such as propynyl or cyclopropenyl; the photoionization onset for the propynyl radical has been calculated to be approximately 11 eV,[21] while the IP for the cyclopropenyl radical is reported to be 6.6 eV.[14] The identity of the C_4H_5 product is discussed in Sec. V.

IV. ANALYSIS

A. Translational energy distributions

For each dissociation channel, the photofragment energy and angular distribution $P(E_T,\theta)$, is given by

$$P(E_T,\theta)=P(E_T)T(\theta),$$

where $P(E_T)$ and $T(\theta)$ are the uncoupled center-of-mass translational energy and angular distributions, respectively. The excimer laser is unpolarized, so with the geometry used in this instrument, in which the laser propagation direction is perpendicular to the plane defined by the molecular beam and the detector, $T(\theta)$ for each channel appears isotropic. We then determine $P(E_T)$ for each channel through forward convolution, in which an assumed $P(E_T)$ distribution is convoluted over the various instrument parameters to simulate the TOF spectra.[22,23] The $P(E_T)$ distribution is adjusted pointwise until the best simultaneous fit of the simulation to the data at all observed angles is obtained.

The $P(E_T)$ distribution used to fit the $C_3H_3+CH_3$ channel is shown in the upper panel in Fig. 5; the calculated laboratory TOF spectra corresponding to this distribution are superimposed on the data in Fig. 2. As can be seen from the figure, the distribution peaks at 5 kcal/mol and extends to approximately 27 kcal/mol, a value well below the maximum translational energy of 69.1 kcal/mol, using the values given in the literature.[19,20]

Since the methyl and propargyl fragments are a momentum-matched pair, only a single $P(E_T)$ distribution should be needed, in principle, to fit the laboratory TOF distributions in Fig. 2 for ions with $m/e=39$ and 15. In fact, at longer flight times there is a small contribution to the $m/e=15$ data from dissociative ionization of the C_3H_3 fragments. Nonetheless, the TOF spectra are dominated by the

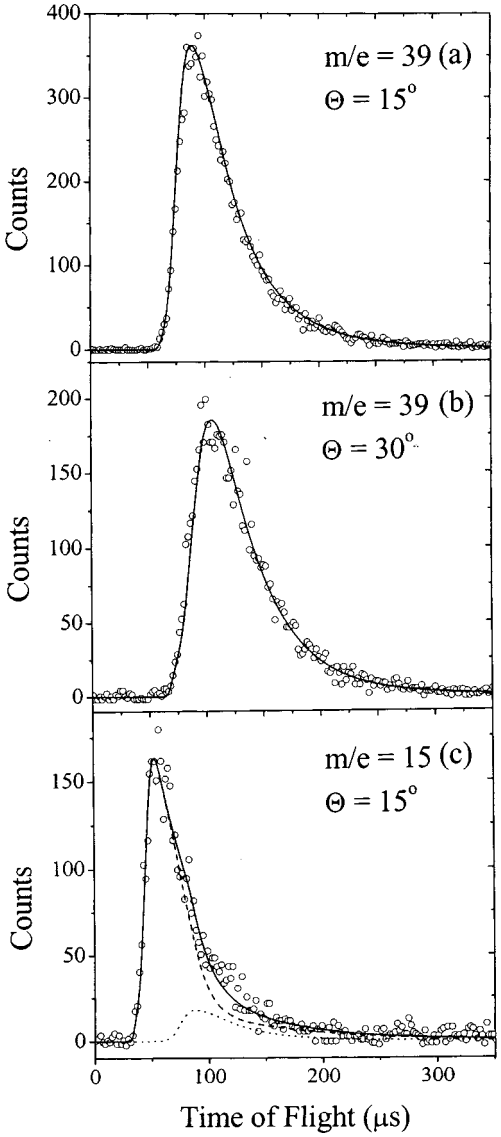

FIG. 2. TOF spectra for $m/e=39(C_3H_3^+)$ at source angles of (a) 15° and (b) 30° using a photoionization energy of 11 eV. The open circles represent the data and the solid line represents the forward convolution fit to the data using the $P(E_T)$ distribution shown in Fig. 5(a). The TOF spectrum for $m/e=15(CH_3^+)$ at a scattering angle of 15° with a photoionization energy of 11 eV is shown in (c) and is fit with the same $P(E_T)$ distribution used to fit (a) and (b). The single-dashed line represents the contribution from $m/e=15$, and the dotted line represents the contribution from dissociative ionization of $m/e=39$, the momentum-matched partner to $m/e=15$. The solid line represents the total forward convolution fit to the data.

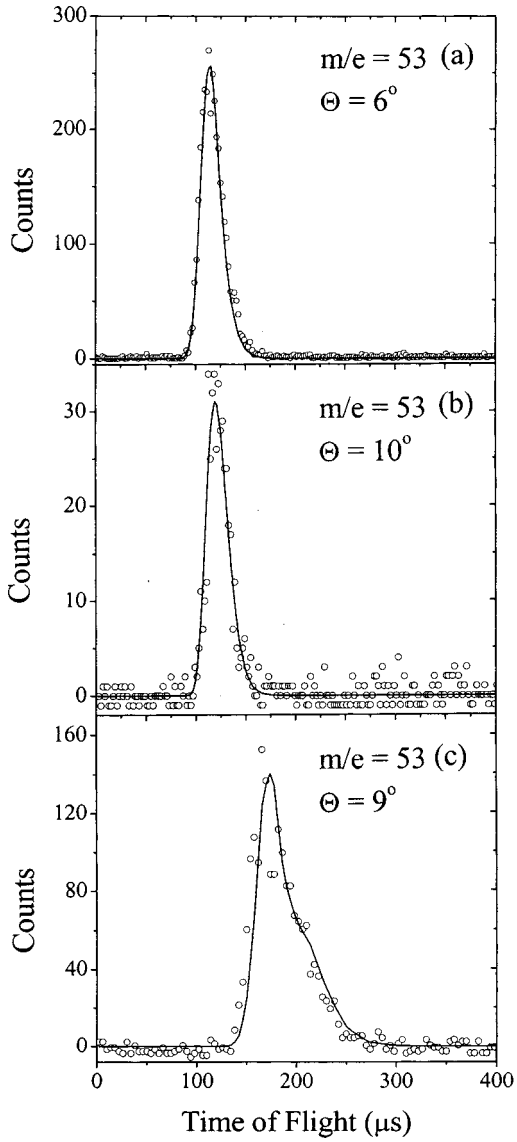

FIG. 3. TOF spectra at source angles of (a) 6° and (b) 10° for $m/e=53(C_4H_5^+)$ from a helium-seeded parent beam, as well as at (c) 9° for $m/e=53(C_4H_5^+)$ from a parent beam seeded in neon. The undulator gap was set to deliver a photoionization energy of 8.5 eV, and the MgF_2 window was in place. The open circles represent the data and the solid line represents the forward convolution fit to the data using the $P(E_T)$ distribution shown in Fig. 5(b).

contribution from parent ions, a direct result of using VUV light rather than electron impact to ionize the scattered photofragments.

The $P(E_T)$ distribution used to fit the C_4H_5+H channel is shown in the lower panel of Fig. 5, with the corresponding calculated laboratory TOF distributions superimposed on the data in Fig. 3. Assuming formation of the most stable C_4H_5 isomer, the 2-butyn-1-yl radical (see Fig. 1), the maximum available energy for this channel is approximately 63.5 kcal/mol. The maximum translational energy in the $P(E_T)$ distribution in Fig. 5, 27 kcal/mol, is well below this value. In order to fit the TOF data for 1,2-butadiene seeded in Ne (bottom panel, Fig. 3), the $P(E_T)$ distribution needed to be sharply truncated at energies below 7 kcal/mol. This truncation, discussed further below, is due to decomposition of slow C_4H_5 fragments.

B. Branching ratio

While it would be desirable to extract a branching ratio for the two product channels R1 and R2, this is somewhat problematic given the $P(E_T)$ distributions. An approximate branching ratio for production of C_3H_3 versus *stable* C_4H_5, i.e., the C_4H_5 that does not dissociate prior to detection, can be obtained from the signal levels in the laboratory TOF spectra, as long as these are normalized to the VUV intensity and number of laser shots. From the fitting program used to generate the TOF spectra, one obtains the relative weights of

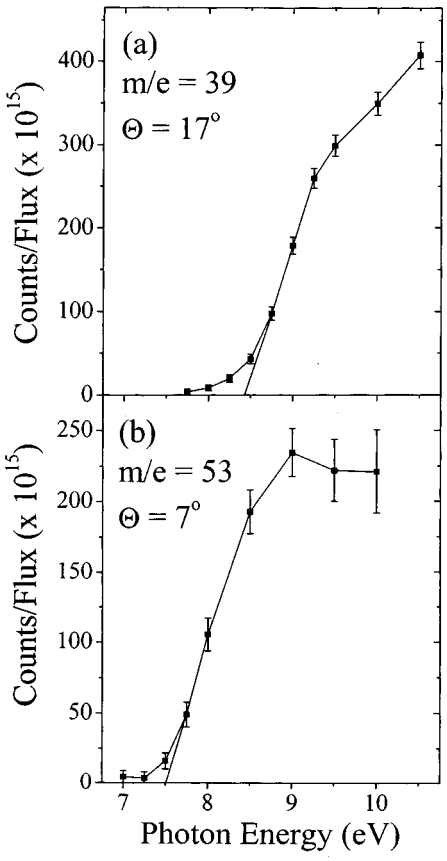

FIG. 4. (a) Photoionization efficiency curve for $m/e=39(C_3H_3^+)$ at a source angle of 17° for photoionization energies of 7.75–10.5 eV, using the MgF_2 window for reduction of residual high-energy tail in the undulator radiation. The squares represent the data points with 2σ error bars. (b) Photoionization efficiency curve for $m/e=53(C_4H_5^+)$ at a source angle of 7° for photoionization energies of 7.0–10.0 eV. The MgF_2 window was in place during data collection.

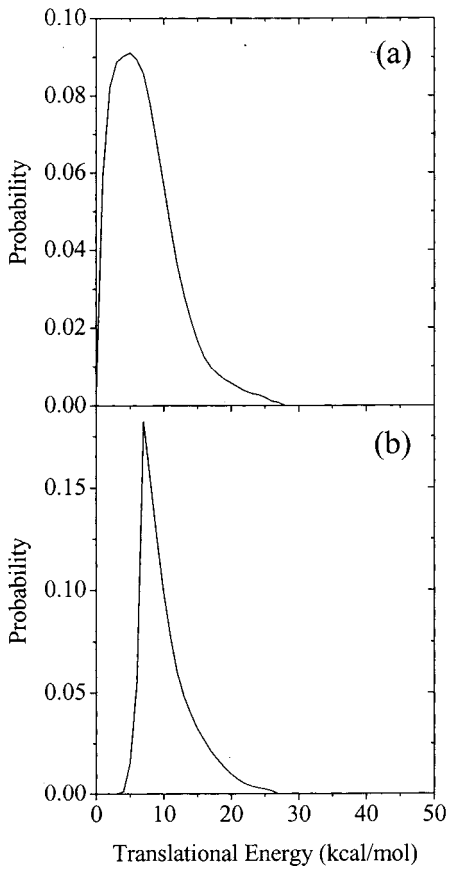

FIG. 5. (a) Center-of-mass (c.m.) translational energy distribution ($P(E_T)$) for methyl loss (R1), where $E_{T,\max}=69.1$ kcal/mol. (b) c.m. translational energy distribution for atomic-hydrogen loss (R2), where $E_{T,\max}=63.5$ kcal/mol.

the $P(E_T)$ distributions needed to reproduce the relative signal intensities of the TOF spectra for the two channels. We used the laboratory TOF data for $m/e=39$ at 11 eV photon energy for C_3H_3 and $m/e=53$ at 8.5 eV photon energy for C_4H_5. This procedure yields a branching ratio of C_3H_3:stable $C_4H_5=96:4$. It is important to note that this is *not* the R1:R2 branching ratio because of the decomposition of the slow C_4H_5 products mentioned above. To obtain a reasonably accurate value for R1:R2 one needs the complete rather than truncated $P(E_T)$ distribution for R2, which could be obtained in principle through TOF of the H atom product; unfortunately the unfavorable kinematics for H atom detection preclude this measurement in the current configuration of the instrument.

These considerations alone would imply that the R1:R2 ratio is considerably smaller than 96:4. However, the accuracy of this ratio, even under the restriction that it applies only to stable C_4H_5, depends on two additional approximations. First, the photoionization cross sections for C_4H_5 at 8.5 eV and C_3H_3 at 11 eV have been assumed to be the same. Even though these photon energies are near or just above where the PIE curves flatten out, there is no information on the absolute values of the cross sections at any energy. We have also implicitly assumed that the two channels have angular distributions with the same anisotropy parameter, β, an assumption that cannot be tested with our experimental arrangement, because the product angular distributions in the plane perpendicular to the laser propagation direction (the detection plane in our case) are isotropic when an unpolarized laser is used regardless of the value of β.

V. DISCUSSION

As shown in Fig. 1, many reaction channels are possible for 1,2-butadiene following 193 nm excitation. However, only two primary channels, R1 and R2, are observed: H atom loss and production of CH_3 + propargyl radical. Both of these are simple bond fission channels. The $P(E_T)$ distributions for both channels peak at low translational energy and drop to zero intensity at translational energies well below the maximum allowed values. The dominant channel, $CH_3+C_3H_3$, lies 7.3 kcal/mol below the lowest C_4H_5+H channel.

This set of observations is consistent with dissociation proceeding via internal conversion to the ground electronic state, followed by statistical decomposition to products. Neither bond fission channel is expected to have an exit barrier with respect to products, so the $P(E_T)$ distributions should peak at very low translational energies if statistical dissociation is occurring, in agreement with experiment. While there

are several other channels at comparable or lower energy relative to R1 and R2 (see Fig. 1), these other channels either require isomerization prior to dissociation or would be expected to have a significant exit barrier with respect to products. For example, 1,2-butadiene would need to isomerize to 1,3-butadiene before producing two vinyl radicals. H atom migration would be necessary for the production of ethylene and C_2H_2. The various H_2 loss channels are likely to involve tight transition states associated with substantial exit barriers; formation of H_2+1,2,3-butatriene, for example, the simplest H_2 loss channel, must proceed through a four-center transition state. Thus, it appears that following excitation at 193 nm, bond fission from 1,2-butadiene in its ground electronic state is significantly faster than these more complex processes.

As noted in the Introduction, thermal experiments on 1,2-butadiene decomposition show evidence for isomerization to 1,3-butadiene.[6,7] In a recent photolysis study of 1,3-butadiene at 193 nm,[24] the production of two vinyl radicals from C–C bond fission as well as the production of $C_2H_4+C_2H_2$ were found to be important channels. The absence of these channels in the 193 nm photolysis of 1,2-butadiene indicates that isomerization from 1,2- to 1,3-butadiene does not occur to any significant extent. The apparent contradiction between the thermal and photolysis experiments on 1,2-butadiene is most likely due to the significantly higher excitation energy of the reactant in our experiment than in the thermal experiments ($T=1100-1600\,\mathrm{K}$), so that bond fission processes, which typically have higher barriers but looser transition states (i.e., higher A factors) than isomerization, can dominate.

While the $CH_3+C_3H_3$ channel is relatively straightforward, there are two interesting aspects of the C_4H_5+H channel worthy of further discussion. The first is the identity of the C_4H_5 radical, for which several isomeric forms are energetically accessible. The energetics of these isomers have been thoroughly explored in theoretical studies by Cooksy and co-workers.[17,25] C–H bond fission from 1,2-butadiene results in three possible C_4H_5 isomers (Fig. 1), listed in order of increasing energy: 2-butyn-1-yl, from cleavage of the secondary C–H bond, 1-butyn-3-yl, from C–H bond fission on the terminal CH_2 group, and 1,2-butadien-4-yl, from loss of a methyl H atom. The 1-butyn-3-yl and 1,2-butadien-4-yl isomers are calculated to lie 2.4 and 3.1 kcal/mol above the 2-butyn-1-yl. The two lower energy isomers are resonance-stabilized with allylic structures.

In any case, if a statistical dissociation mechanism is operative, then 2-butyn-1-yl should be the favored C_4H_5 species, although the other two isomers are low-lying enough so that they, too, are likely to be formed to some extent. Moreover, the C_4H_5 radical is formed with significant internal energy; according to the $P(E_T)$ distribution, none of this product is formed with less than 36 kcal/mol of internal energy. Hence, isomerization may occur among these low-lying isomers and even some higher-lying structures (e.g., a cyclic isomer is calculated to lie only 4.1 kcal/mol above the 2-butyn-1-yl isomer), depending on the isomerization barrier heights. The only reported experimental values of IP's for C_4H_5 isomers (obtained from appearance potentials) are 7.97 eV for 1-butyn-3-yl and 7.95 eV for 2-butyn-1-yl.[26] Our measured IP of 7.5 ± 0.2 eV for the C_4H_5 product is slightly below these two values, as one would expect if these two isomers were formed in our experiment with enough vibrational excitation to lower their ionization thresholds. However, since experimental IP's are unavailable for the other C_4H_5 isomers, their presence cannot be ruled out based on our PIE curve.

The second noteworthy issue regarding this channel is that it was necessary to sharply truncate the $P(E_T)$ distribution below 7 kcal/mol in order to fit the Ne-seeded TOF data for $m/e=53$. This truncation indicates that C_4H_5 fragments with $E_T<7$ kcal/mol have enough internal energy to undergo further dissociation and hence are not detected. A similar effect has been seen for other molecules where photodissociation produces an atom and a molecular fragment, e.g., C_2F_4Br from 1,2-C_2F_4BrI dissociation at 266 nm[27] and CH_3CO from the 248 nm dissociation of acetyl chloride.[28] In our experiment, this secondary dissociation process cannot be identified unambiguously if a He-seeded beam is used, because the slow fragments are confined to small laboratory scattering angles where they are difficult to observe without raising the pressure in the detector region above acceptable operating levels. Assuming 7 kcal/mol goes into translation of the products, the maximum angle that $m/e=53$ products would be expected to be seen is $\Theta_{LAB}=6.4°$ for the helium expansion. In contrast, for a slower, Ne-seeded beam, the maximum angle to see C_4H_5 products with 7 kcal/mol translational energy release is $\Theta_{LAB}=10.3°$. Additionally, using a beam seeded in neon spreads out the TOF spectrum, making features in the TOF spectrum more distinguishable.

According to the heats of formation used to construct Fig. 1, at 193 nm excitation the photon energy exceeds that needed for production of vinylacetylene (C_4H_4)+2H and $C_2H_3+C_2H_2+H$ by 10.7 and 8.3 kcal/mol, respectively. Hence, C_4H_5 products with $E_T<10.7$ kcal/mol will have enough energy to dissociate to C_4H_4+H, and those formed with $E_T<8.3$ kcal/mol can dissociate to $C_2H_3+C_2H_2$. Both values lie near the truncation point at 7 kcal/mol in the $P(E_T)$ distribution for C_4H_5, so either channel is a reasonable candidate for secondary dissociation of C_4H_5. It should in principle be possible to observe the secondary dissociation products directly. Using a He-seeded beam, we saw a small amount of $m/e=52(C_4H_4)$ products close to the beam, but not enough signal to analyze quantitatively. No $m/e=52$ products were observed with a Ne-seeded beam, which may reflect the lower signal levels associated with Ne seeding because the products are spread over a larger range of laboratory angles. Some signal at $m/e=26$ was seen, but essentially nothing at $m/e=27$, and a power dependence study of the $m/e=26$ signal indicated that it primarily resulted from a two-photon process. None of the three C_4H_5 isomers in Fig. 1 can dissociate to $C_2H_3+C_2H_2$ by simple bond fission, while vinylacetylene+H can result from C–H bond fission from the two higher energy isomers. Based on these observations and considerations, we tentatively claim vinylacetylene+H to be the secondary dissociation channel.

ACKNOWLEDGMENTS

The authors would like to acknowledge Professor Tomas Baer and Dr. Arthur G. Suits for permitting use of End Station 1 on the Chemical Dynamics Beamline, and Dr. O. Sorkhabi for support during the initial experiments. This work was supported by the Director, Office of Basic Energy Sciences, Chemical Sciences Division of the U. S. Department of Energy under Contract No. DE AC03-76SF00098.

[1] R. Schinke, *Photodissociation Dynamics* (University Press, Cambridge, 1993).
[2] J. Collin and F. P. Lossing, Can. J. Chem. **35**, 778 (1957).
[3] R. D. Doepker and K. L. Hill, J. Phys. Chem. **73**, 1313 (1969).
[4] Z. Diaz and R. D. Doepker, J. Phys. Chem. **81**, 1442 (1977).
[5] C. H. Wu and R. D. Kern, J. Phys. Chem. **91**, 6291 (1987).
[6] R. D. Kern, H. J. Singh, and C. H. Wu, Int. J. Chem. Kinet. **20**, 731 (1988).
[7] Y. Hidaka, T. Higashihara, N. Ninomiya, T. Oki, and H. Kawano, Int. J. Chem. Kinet. **27**, 331 (1995).
[8] D. A. Blank, Ph.D. thesis, University of California, Berkeley, 1997.
[9] X. Yang, D. A. Blank, J. Lin, A. M. Wodtke, A. G. Suits, and Y. T. Lee, Rev. Sci. Instrum. **68**, 3317 (1997).
[10] P. A. Heimann, M. Koike, C. W. Hsu, M. Evans, C. Y. Ng, D. Blank, X. M. Yang, C. Flaim, A. G. Suits, and Y. T. Lee, *SPIE Proceedings*, Vol. 2856, 1996, pp. 90–99.
[11] M. Koike, P. A. Heimann, A. H. Kung, T. Namioka, R. Digennaro, B. Gee, and N. Yu, Nucl. Instrum. Methods Phys. Res. A **347**, 282 (1994).
[12] A. G. Suits, P. Heimann, X. M. Yang, M. Evans, C. W. Hsu, K. T. Lu, Y. T. Lee, and A. H. Kung, Rev. Sci. Instrum. **66**, 4841 (1995).
[13] T. T. Nguyen and K. D. King, Int. J. Chem. Kinet. **14**, 613 (1982).
[14] S. G. Lias, J. E. Bartmas, J. F. Liebman, J. L. Holmes, R. D. Levin, and W. G. Mallard, J. Phys. Chem. Ref. Data **117**, (1988).
[15] K. M. Ervin, S. Gronert, S. E. Barlow, M. K. Gilles, A. G. Harrison, V. M. Bierbaum, C. H. DePuy, W. C. Lineberger, and G. B. Ellison, J. Am. Chem. Soc. **112**, 5750 (1990).
[16] J. A. Miller and C. F. Melius, Combust. Flame **91**, 21 (1992).
[17] C. L. Parker and A. L. Cooksy, J. Phys. Chem. A **103**, 2160 (1999).
[18] M. S. Robinson, M. L. Polak, V. M. Bierbaum, C. H. DePuy, and W. C. Lineberger, J. Am. Chem. Soc. **117**, 6766 (1995).
[19] T. Gilbert, R. Pfab, I. Fischer, and P. Chen, J. Chem. Phys. **112**, 2575 (2000).
[20] NIST Chemistry Webbook, 2000.
[21] W. Sun, K. Yokoyama, J. C. Robinson, A. G. Suits, and D. M. Neumark, J. Chem. Phys. **110**, 4363 (1999).
[22] X. Zhao, Ph.D. thesis, University of California, Berkeley, 1989.
[23] J. D. Myers, Ph.D. thesis, University of California, Berkeley, 1993.
[24] J. C. Robinson, W. Sun, S. A. Harris, F. Qi, and D. M. Neumark (in preparation).
[25] C. L. Parker and A. L. Cooksy, J. Phys. Chem. A **102**, 6186 (1998).
[26] F. P. Lossing and J. L. Holmes, J. Am. Chem. Soc. **106**, 6917 (1984).
[27] D. Krajnovich, L. J. Butler, and Y. T. Lee, J. Chem. Phys. **81**, 3031 (1984).
[28] S. North, D. A. Blank, and Y. T. Lee, Chem. Phys. Lett. **224**, 38 (1994).